

# Lower-dimensional projections of cellular expression improves cell type classification from single-cell RNA sequencing

Muhammad Umar,<sup>1</sup> Muhammad Asif<sup>2</sup> and Arif Mahmood<sup>1,\*</sup>

<sup>1</sup>Department of Computer Science, Information Technology University (ITU), Ferozepur Road, 56700, Lahore, Pakistan and <sup>2</sup>Department of Bio-informatics and Biotechnology, Government College University, Allama Iqbal Road, 38000, Faisalabad, Pakistan

\*Corresponding author. arif.mahmood@itu.edu.pk

## Abstract

Single-cell RNA sequencing (scRNA-seq) enables the study of cellular diversity at single cell level. It provides a global view of cell-type specification during the onset of biological mechanisms such as developmental processes and human organogenesis. Various statistical, machine and deep learning-based methods have been proposed for cell-type classification. Most of the methods utilizes unsupervised lower dimensional projections obtained from for a large reference data. In this work, we proposed a reference-based method for cell type classification, called EnProCell. The EnProCell, first, computes lower dimensional projections that capture both the high variance and class separability through an ensemble of principle component analysis and multiple discriminant analysis. In the second phase, EnProCell trains a deep neural network on the lower dimensional representation of data to classify cell types. The proposed method outperformed the existing state-of-the-art methods when tested on four different data sets produced from different single-cell sequencing technologies. The EnProCell showed higher accuracy (98.91) and F1 score (98.64) than other methods for predicting reference from reference datasets. Similarly, EnProCell also showed better performance than existing methods in predicting cell types for data with unknown cell types (query) from reference datasets (accuracy:99.52; F1 score: 99.07). In addition to improved performance, the proposed methodology is simple and does not require more computational resources and time. the EnProCell is available at <https://github.com/umar1196/EnProCell>.

**Key words:** scRNA classification, Dimension reduction, Machine Learning, Projections, Data Science

## Introduction

Single-cell RNA sequencing (scRNA-seq) revolutionized the understanding of cellular expression by providing a static and high-resolution snapshot of gene expression at the individual cell level. Unlike the traditional bulk RNA-seq, scRNA-seq enables researchers to comprehensively characterize cellular heterogeneity(1), thus, making it a powerful tool to investigate the response to therapy(2), the likelihood of resistance(3; 4), candidacy for alternative therapeutic intervention(5), evolution of the human brain(6; 7) and understanding of changes in cellular state because of development or response to certain stimuli(8; 9). Additionally, scRNA showed applications in the identification of novel cell types and subtypes(10; 11), the discovery of rare cells(12; 13; 6), and the elucidation of complex tissue architectures, including the human brain(14). The identification of cell types or states is a primary objective of scRNA-seq studies(15), as the discovery of accurate cell representations contributes significantly to our understanding of cellular heterogeneity and its implications in biological systems.

Therefore to decipher the cell types or states from single cell gene expression profiles, different data analytical approaches such as correlation(16) and machine learning(17; 18; 19) based method have been proposed. Despite these efforts, cell type identification remains an elusive task due to a number of challenges.

scRNA experiments produce a large amount of sparse and high-dimensional data. Dimension reduction methods such as the principal component analysis (PCA) recapitulate biologically relevant information from sparse and high dimensional cellular expression. Clustering is employed to identify biologically similar groups of cells or states. There exist several methods for clustering of cells such as SC3 (20), Seurat(21), and pcaReduce (22). The annotation of clusters is largely determined by identifying differentially expressed genes for each cluster. To define the cell type for each identified cluster, differentially expressed genes of targeted cluster are searched in canonical gene-based marker databases (23; 24; 25). The availability of cell atlas, for example, Human Cell Atlas (HCA) motivated the development of cell-type annotation approaches that leverage the previously annotated reference data. Such reference-based approaches transfer cell type labels from reference to data with unknown cell types by computing the similarities between them. There also exist methods that leverage the lower dimensional projections of reference data to predict the cell type for query (unannotated scRNA data). For example, scPred(17) employs single value decomposition (SVD) to compute principal components (PCs), representing cellular expression in lower dimensions. Wilcoxon test was employed to identify PCs differentiating the cell types. Support vector machine (SVM) was employed on selected features to predict the cell types. Furthermore, the query dataset was also projected in lower dimensional space to predict their cell

types by utilizing reference data. Another widely used method, SingleR(16) is based on a correlation approach. To recognize type of cells, it estimates the correlation between the cellular expression of reference and query data.

ACTINN (Automated Cell Type Identification using Neural Networks)(19) does not include lower dimension projections, instead, it employs popular neural networks to assign cell types to test data. Multiple hidden layers were created and output nodes were equal to the number of cell types in reference data. Transfer learning utilizes the classifiers previously trained on similar data to label unknown data instances(26). Lieberman et al. proposed a transfer-learning framework, called CaSTLe (18), which first applies feature engineering which is followed by the utilization of pre-trained XGBoost(27). CaSTLe feature engineering consists of a screening of genes with higher mean expression and mutual information gain. It also excludes correlated genes and assigns different ranges to the resultant data by using the pre-defined ranges. Recent technologies are accelerating the production of large and accurate datasets.

Transfer learning-based classifiers lacking recent data may result in limited performance and can reduce the biological understanding of an underlying phenomenon. Correlation-based approaches may have limited biological insights due to the similarity in gene expression of different cell types. The lack of markers for several cell types limits the applicability of marker-based approaches.

Furthermore, clustering heavily relies on lower dimensional projections obtained by employing PCA. The PCA aims to find the orthogonal directions that capture the maximum variance but does not ensure the separability of classes. The feature vectors that are linearly separable in higher dimensional space get mixed in the lower dimensional space. This limitation becomes further complex when the classification of cell type is based on projections obtained from solely unsupervised methods, thus limiting the biological interpretability of identified clusters(28).

In this study, we proposed a simple reference-based method for cell type classification, named as EnProCell. It also obtained lower dimensional projection using PCA. However, to include the class information in the dimension reduction phase, PCA was ensemble with Multiple Discriminant Analysis (MDA). The components extracted using the PCA and MDA were used to train a classifier. MDA is a dimension reduction technique with an advantage of clear separation of cell types in the lower dimensional space. Herein, we combined the strengths of both techniques capturing the components with the highest variance and components ensuring class separability in the case of PCA and MDA respectively, resulting in improved performance compared to other state-of-the-art methods. To ensure the generalizability of the method along with reference data we also tested the performance of the classifier on query data.

## Materials and methods

Figure 1 presents a graphical overview of the proposed methodology.

### Data preprocessing and normalization

First, single cell gene expression profiles were screened for variable genes. Variable genes have a significant difference in expression level in the cells. These genes have a high variance

as compared to other genes in the data and show high cell-to-cell variations. To select the variable genes for each cell, mean expression and variance were calculated for all cells, and the genes with the high variance-to-mean ratio were selected for further analysis. Furthermore, cell expression profiles were scaled and normalized with log-transformed. Seurat R package was used for preprocessing and normalization.

### EnProCell

The proposed method (EnProCell) is based on two steps. In the first step, a model is trained using the training data set consisting of gene expression matrix  $X_{train}$ , consisting of  $n$  training examples and  $m$  genes. In the second step trained model is used to predict the cell type of test data set from different samples. In training principle component analysis is used to find the components with the high variance that are combined with the discriminative components using the multiple discriminant analysis. Combined components are used to project the training data to lower dimensional space and the model is trained using this reduced form of data. To predict the cell types, test data expression values are projected to lower dimensional space using the components from a training set and fed to the trained model to assign the cell types.

#### *Extracting the principle components (PCs) with high variance*

To extract the principle components with high variance pre-processed gene expression matrix  $X_{train}$  is used, consisting of  $n$  records and  $m$  genes. To center the expression matrix  $X$  for each gene, the mean expression value is calculated and subtracted from each expression value.

$$\mu = \frac{1}{n} \sum_{i=1}^n x_i \quad (1)$$

$$X_{nm} = \begin{bmatrix} x_{11} - \mu_1 & x_{12} - \mu_2 & \dots & x_{1m} - \mu_m \\ x_{21} - \mu_1 & x_{22} - \mu_2 & \dots & x_{2m} - \mu_m \\ \vdots & \vdots & \ddots & \vdots \\ x_{n1} - \mu_1 & x_{n2} - \mu_2 & \dots & x_{nm} - \mu_m \end{bmatrix}$$

After this covariance matrix,  $C$  is calculated, which measures how a change in one variable affects the other variables. The mathematical expression is given as:

$$C_{nn} = X_{nm}^T * X_{nm} \quad (2)$$

$$C_{mm} = \begin{bmatrix} C(x_{11}, x_{11}) & C(x_{12}, x_{22}) & \dots & C(x_{1m}, x_{mm}) \\ C(x_{21}, x_{11}) & C(x_{22}, x_{22}) & \dots & C(x_{2m}, x_{mm}) \\ \vdots & \vdots & \ddots & \vdots \\ C(x_{m1}, x_{11}) & C(x_{m2}, x_{22}) & \dots & C(x_{mm}, x_{mm}) \end{bmatrix}$$

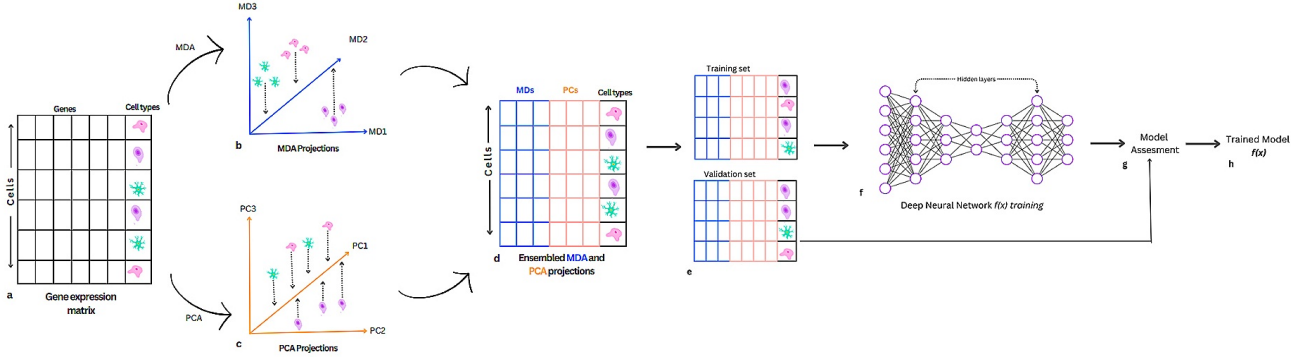


**Fig. 1.** Workflow of EnProCell methodology. **a** Training phase. The gene expression matrix consists of gene expression values in different cells. **a** MDA is applied to obtain directions in lower dimensional space that ensure the class separability in lower dimensional space. **c** PCA is employed to obtain the high-variance components. **d** Projections obtained from MDA and PCA are ensembled to obtain a single matrix used for classification. **e** Ensembled matrix is split into a train and validation set. **f** A deep neural network  $f(x)$  consisting of five hidden layers having the auto-encoder-like architecture is trained using the training data. **g** Model is assessed using the validation set during training to avoid over-fitting. **h** Trained model  $f(x)$  is saved.

The eigenvalue equation is solved to get the eigenvectors of the covariance matrix. First, the eigenvalues are found and the eigenvectors corresponding to the maximum eigenvalues are found. The eigenvalue equation to get the eigenvector is given as:

$$CP = \lambda P \quad (3)$$

where  $A$  is the co-variance matrix,  $P$  is the eigenvector and  $\lambda$  is the eigenvalue corresponding to eigenvector  $P$ .

After calculating the eigenvectors and eigenvalues, eigenvectors are sorted in descending order, and vectors associated with the high eigenvalues are selected as they capture the high variance in data. The matrix  $u$  having the  $l$  components with high variance from the matrix  $P$  for the  $X_{train}$  is represented as:

$$U_{ml} = \begin{bmatrix} u_{11} & u_{12} & \dots & u_{1l} \\ u_{21} & u_{22} & \dots & u_{2l} \\ \vdots & \vdots & \ddots & \vdots \\ u_{m1} & u_{m2} & \dots & u_{ml} \end{bmatrix}$$

### Extracting the discriminative components

To deal with the limitation of principle component analysis, that is when the data is projected to lower dimensional space the data for different classes overlap. To ensure the separability in the lower dimensional space Multiple discriminant analysis is used, which tries to maximize the inter-class scatter and reduces the intra-class scatter that increases the separability in the lower dimensional space. To calculate the between-class scatter, the mean for each class is calculated and then for each class difference of mean is calculated, and multiplied by its transpose. The mathematical form is given as

$$S_b = (m_1 - m_2)(m_1 - m_2)^T \quad (4)$$

Here  $m_1$  and  $m_2$  refer to the means of class 1 and 2 respectively.

To calculate the within-class scatter mean vector for each class is calculated. Then the mean of each class is subtracted from the respective class data and the resultant matrix is multiplied by the transpose of itself to obtain the square matrix. This square matrix captures the variability or scatter within a class. Scatter matrices obtained from each class are added up to get a single matrix that captures the within-class scatter in

data. The mathematical expression is given as

$$S_w = \sum (X_i - m_i)(X_i - m_i)^T \quad (5)$$

Here  $X_i$  refers to data points of class  $i$ ,  $m_i$  is the mean of that  $i$ th class and  $S_w$  represents the within-class scatter matrix.

After computing the between-class and within-class scatter matrices, the generalized eigenvalue problem is solved to obtain the discriminant components. In mathematical form, it is given as

$$S_w^{-1} * S_b * V = \lambda * V \quad (6)$$

Where  $S_w^{-1}$  is the inverse of the within-class scatter matrix,  $\lambda$  is the eigenvalues and  $V$  is the matrix of eigenvectors. These vectors are sorted in descending order and the number of components selected is equal to the number of unique classes in the dataset.

In the case of a dataset containing the  $k$  unique classes and  $n$  number of records the matrix for the discriminative components can be represented as:

$$V_{mk} = \begin{bmatrix} v_{11} & v_{12} & \dots & v_{1k} \\ v_{21} & v_{22} & \dots & v_{2k} \\ \vdots & \vdots & \ddots & \vdots \\ v_{m1} & v_{m2} & \dots & v_{mk} \end{bmatrix}$$

### Model Training

After obtaining the discriminative components and the components with the high variance, they are ensembled together. Ensembled representation  $S$  is given as

$$S_{mj} = [VU]$$

or

$$S_{mj} = \begin{bmatrix} v_{11} & v_{12} & \dots & v_{1k} & u_{11} & u_{12} & \dots & u_{1l} \\ v_{21} & v_{22} & \dots & v_{2k} & u_{21} & u_{22} & \dots & u_{2l} \\ \vdots & \vdots & \ddots & \vdots & \vdots & \vdots & \ddots & \vdots \\ v_{m1} & v_{m2} & \dots & v_{mk} & u_{m1} & u_{m2} & \dots & u_{ml} \end{bmatrix}$$

$S$  is a  $n$  by  $j$  dimensional vector where  $n$  is the number of rows and  $j$  is the sum of  $k$  and  $l$ . This ensemble representation is

**Table 1.** Datasets used in the study.

Name	Protocol/Platform	Tissue	No. of Cells	No. of Genes	No. of Cell types
Xin	SMARTer	Pancrease	1449	33890	4
Baron	inDrop	Pancrease	8569	17500	14
Muraro	CEL-Seq2	Pancrease	2122	18916	9
Seegerstolpe	Smart-Seq2	Pancrease	2133	22758	12
PBMC1	NovaSeq 6000, MGISEQ-2000	Blood	3500	32838	9
PBMC2	NovaSeq 6000, MGISEQ-2000	Blood	3000	32838	9

used to project the  $X_{nm}$  into lower dimensional space.

$$P_{nj} = X_{nm} * S_{mj} \quad (7)$$

Here  $P$  is the lower dimensional representation of training data and it is further used for training of simple neural network consisting of a hidden layer and an output layer. The output of 5 hidden layers  $H$  is defined as

$$H = \sigma(W^5 * \sigma(W^4 * \sigma(W^3 * \sigma(W^2 * \sigma(W^1 * P + b^1) + b^2) + b^3) + b^4) + b^5) \quad (8)$$

Where  $P$  is the input matrix, which is the lower dimensional representation of the training data using the ensemble components,  $W^1, W^2, W^3, W^4, W^5$  and  $b^1, b^2, b^3, b^4, b^5$  are the weights and biases for the first, second, third, fourth and fifth hidden layers respectively.  $\sigma(\cdot) = RELU(\cdot)$  is the non-linear activation function. The representation of the output of the proposed model is

$$\hat{Y} = softmax(HW^{(o)} + b^{(o)}) \quad (9)$$

Where  $W^{(o)}$  and  $b^{(o)}$  are the weight and biases for the output layer and  $softmax$  is the activation function and  $\hat{Y}$  represents the predictions.

In model training, the goal is to minimize the cross entropy loss between the ground truth labels and predicted labels. The objective function that is optimized is given as

$$J = -\frac{1}{N} \left( \sum_{i=1}^N \sum_{j=1}^J y_{ij} \cdot \log(\hat{y}_{ij}) \right) \quad (10)$$

Where  $N$  represents the total number of training examples and  $y_{ij}$  and  $\hat{y}_{ij}$  represents the actual label and predicted cell type probability that the  $i$ th record belongs to class  $j$ .

### Cell labels prediction

Test data gene expression matrix containing the  $q$  records and 2000 variable genes. This matrix is represented as  $T_{qm}$  and is also projected to lower dimensional space using the same ensemble components that were used to project the training data.

$$\hat{P}_{qj} = T_{qm} * S_{mj} \quad (11)$$

Then this lower dimensional representation is used by the trained neural network to predict the cell type.

## Results

In this study, we have proposed a deep learning-based methodology, called EnProCell to further improve the cell type

classification from single-cell expression profiles. EnProCell consists of two core steps. In the first step, EnProCell employs an ensemble of PCA and MDA to obtain a high variance and cell-type separable lower-dimensional projections from scRNA expression matrix. In the second step, these projections are subject to a deep neural network for cell-type classification. Figure 1 shows the workflow of EnProCell.

PCA has been widely employed to obtain the lower dimensional projections of scRNA expression profiles (29; 30). These projections are used either for clustering of similar cells (31) or cell type classification(32). However, PCA is an unsupervised dimensional reduction method. Therefore, in the case of the multi-class classification task, the lower dimensional projections from PCA lack the known cell type information. This limitation may result in overlapping of different cell types while projecting them on components, consequently, affecting the overall performance of machine learning classifiers trained on unsupervised projections. To include the cell type information in the lower dimensional projections, we have applied MDA to scRNA expression profiles. The lower dimensional projections obtained from supervised MDA were ensemble with PCA projections and are used to project the train and test data in lower dimensional space. A deep neural network trained on training data can be used to predict the cell types for test dataset.

The EnProCell was tested on six different datasets (Table 1). The filtered BaronHuman (33) dataset (GEO: GSE84133) was sequenced through inDrop platform and consists of 8569 cells and 17500 genes. The second pancreatic dataset is Muraro (34) sequenced using CEL-Seq2 platform. The filtered pancreatic dataset contains 2122 cells and 18916 genes. The third dataset, Seegerstolpe (35) dataset comprises 2133 cells and 22758 genes after applying the filtration steps. It was sequenced through the Smart-Seq2 sequencing platform. The fourth dataset is Xin (36) which is publically available on GEO having the access number GSE81608. It contains 33890 genes and 1449 cells in filtered form. Furthermore, the most widely used and popular peripheral blood mononuclear cells (PBMCs) data from two different individuals were also used to test EnProCell. Cells were sequenced using Illumina NextSeq 500. The PBMC1 (37) dataset consists of 3500 cells and 32838 genes. The second dataset PBMC2 (37) consists of 3000 cells and 32838 genes, having 9 unique cell types.

F1 score and overall accuracy evaluation measures were used to estimate the performance of EnProCell and other methods on selected datasets. Furthermore, the methods were compared on their ability to accurately classify cell types from the same reference data set, named reference to reference prediction or intra-dataset classification in this manuscript. In intra-dataset

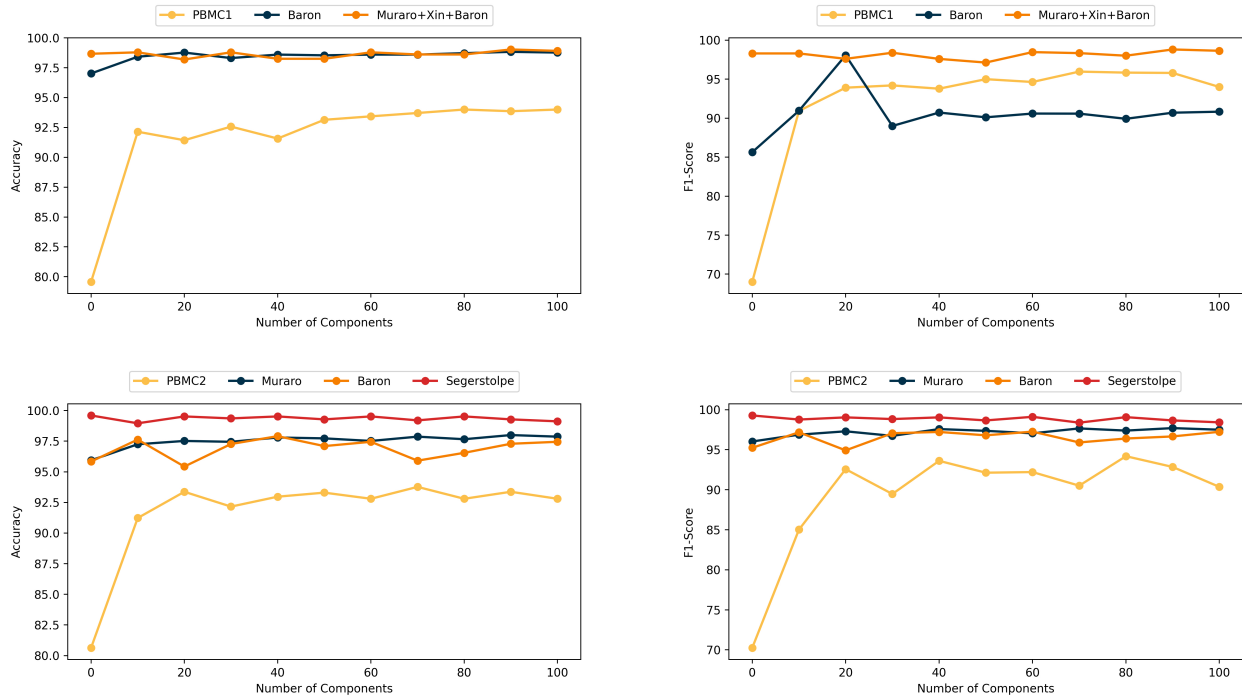


**Fig. 2.** Accuracy and F1 by changing the number of components. (a) Line plot showing the variation in accuracy by changing the number of principal components in reference to reference prediction. (b) Plot to show the effect of varying the number of principal components on the F1 score for reference to reference prediction. (c) Accuracy of predicting the query data by using the different number of components. Query data is shown in the legend. (d) F1 score of reference to query prediction by varying the number of principal components.

classification, both training and test records belong to one reference dataset. Additionally, the robustness of methods in classifying query datasets, never used in the training or testing phase was also assessed. Prediction of cell types for query data from a classifier trained solely on reference is referred as a reference to query prediction or inter-dataset classification.

Before the analysis, selected datasets were subject to data preprocessing and normalization, resulting in the screening of 2000 highly variable genes.

### EnProCell robustness: Evaluating the model performance by changing the number of principal components

To investigate the effect of lower-dimension projections on overall cell types classification, lower-dimension projections from PCA and MDA were computed. In case of MDA, the number of selected components were equal to the number of unique cell types present in the training data. However, a different number of PCs were selected from PCA each time, which were combined with the MDA components, and their impact on cell types classification was explored. This iterative processing was performed on both the scenarios of intra and inter-dataset classification. Figure 2 shows the effect of changing the number of principal components on the accuracy and F1 score of the classifier for intra and inter-data sets classification.

In case of intra-data classification for PBMC1 data, there was a significant increase in the used evaluation measures when the MDA components were ensembled with the PCA components (Figure 2(a) and 2(b)). The accuracy and F1

score was 79.57 and 69.01 respectively when only the MDA components were used. The classifier perform well at 100 PCs where the accuracy was 94.00% (Figure 2(a)) with a 95.84% F1 score (Figure 2(b)). The model also showed better performance at 70 and 80 components. For Baron, dataset accuracy was 97.02 and the F1 score was 85.64 without PCs components. The inclusion of PCA components resulted in improved classification of cell types (accuracy=98.77% and F1 score=98.06%). For the third experiment in which Xin, Baron, and Muraro datasets were combined, the classifier also showed improved performance when 100 PCs were combined with MDA components (accuracy=98.91% and F1 score=98.64%). Without PCA components accuracy and F1 score were 98.67 and 98.30 percent, respectively. All the results for reference to reference prediction scenario are shown in Figures 2(a) and 2(b).

For inter-dataset classification without any PCA component, the accuracy and F1 score were 80.63% and 70.25%, respectively while using the PBMC2 as the query and PBMC1 as reference. By combining the 90 PCA components the accuracy improved to 93.37% (Figure 2(c)) and the F1 score to 92.85% (Figure 2(d)). While using the Baron as the query data and the combination of the other three datasets as the reference the accuracy (97.91%) and F1 score (97.22%) were higher as compared to the accuracy (95.84%) and F1 score (97.22%) when no PCA component was included. When Muraro was used as the query data set the model showed an improvement in evaluation measure by ensembling the 90 PCA components with MDA components referring to Figure 2(c) and 2(d). In predicting the Segerstolpe data the addition of

**Table 2.** Accuracy & F1 score on test set of PBMC1 data using different NN architecture.

Neural-Network(NN) Configuration	Number of hidden layers	Number of nodes	Accuracy	F1
Network 1	2	64, 16	93.29	95.63
Network 2	3	64, 32, 16	93.00	94.45
Network 3	2	100, 55	94.29	95.69
Network 4	3	100, 55, 30	93.86	84.63
Network 5	5	64, 32, 16, 32, 64	93.86	94.02
Network 6	5	100, 55, 30, 55, 100	94.00	95.84

PCA components showed equal performance to the model that is trained on the MDA components only.

These experiments showed that an ensemble of MDA and PCA lower dimensional projections improved the cell type classification.

### Effect of neural network architecture on cell type classification

The neural network presents a complex architecture, which may easily under or overfit for cell-type classification tasks. To avoid the under and overfitting and to ensure generalizability, different architectures of the neural network were tested on the PBMC1 data set. Multiple architectures of the neural network were evaluated on training and validation data and loss curves are drawn for 6 different architectures (Figure 3).

These curves were plotted using the 20% of training data as the validation set. Each model configuration was trained at 100 epochs and using the 100 PCs and 9 components extracted from MDA (equal to the number of unique cell types for the targeted data). Accuracy and F1 score for the test data was also computed to test the generalizability of each architecture of the model (Table 2). Table 2 shows the different neural network architectures, first two architectures, Network 1 and Network 2, consist of two layers with nodes 64, 16 and 64, 32, 16 nodes respectively. The Networks (Network 3 and Network 4) having a more number of nodes showed better accuracy and F1 score compared to the lower number of nodes network (Network 1, Network 2), but Network 4 has a minimum F1 score compared to other networks.

The architecture of network 5 and 6 resembles with autoencoder but the number of nodes were higher in each hidden layer of network 6. The F1 score of network 6 was higher compared to other networks, showing that model predicted the fewer false positives and false negatives. The loss curves for the training and validation data are shown in Figure 3. Network 3 has the lowest validation loss but the model is too simple and has a smaller F1 score compared to Network 6. Although the accuracy of Network 3 is slightly higher than Network 6 having the highest F1 score motivated us to select this architecture for further analysis as the F1 score is a better evaluation measure for classification problems as compared to accuracy. The results presented throughout the manuscript were computed by employing network 6 architecture.

### Performance comparison of EnProCell with existing methods

The performance of EnProCell was compared with already available and widely used classification methods such as ACTINN (19), CaSTLe (18), singleR (16), and scPred (17). These methods are based on different data analytical

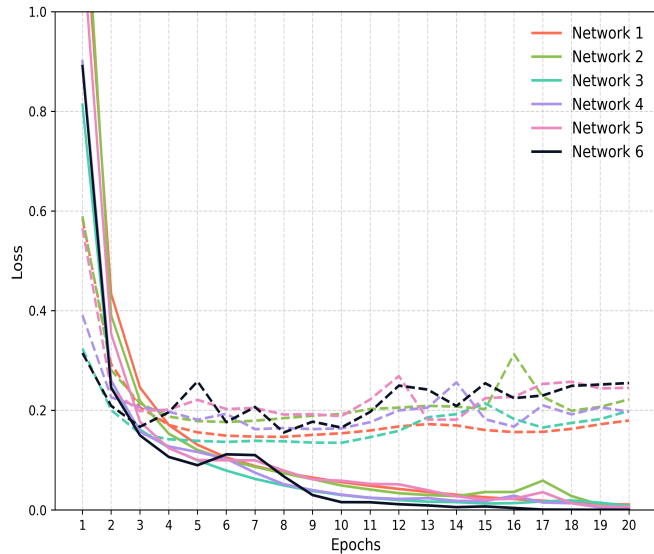


**Fig. 3.** Train and Validation loss curves of different neural network architectures. Validation loss is represented by the dotted line. Curves are generated using the PBMC1 dataset.

techniques. For example, ACTINN employs a popular multi-layer neural network, singleR uses a correlation-based technique with iterative tuning, scPred applies SVD and SVM for cell type classifications, and lastly, CaSTLe is a transfer learning-based method. The motivation for the selection of these methods was to compare EnProCell with different data analytical techniques developed over time. The performance of EnProCell was tested and compared on 6 different datasets (Table 1). To ensure the robustness of the proposed approach across different sequencing platforms, the datasets used were obtained from different sequencing protocols/protocols. All the datasets were from human samples.

### Reference to reference prediction

The performance of EnProCell and other state-of-the-art methods in predicting the subset of reference data from reference (intra-data) was estimated on three different datasets separately (PBMC1, Baron, and combined Muraro, Xin, and Baron). For this purpose, 80% of the data was used for training, and the remaining 20% was used for testing. Figures 4(a) and 4(b) show the performance of EnProCell and other classification methods. Overall, SingleR, CaSTLe, and EnProCell outperformed the scPred and ACTINN. Specifically, EnProCell achieved the highest accuracy (93.71%) and F1

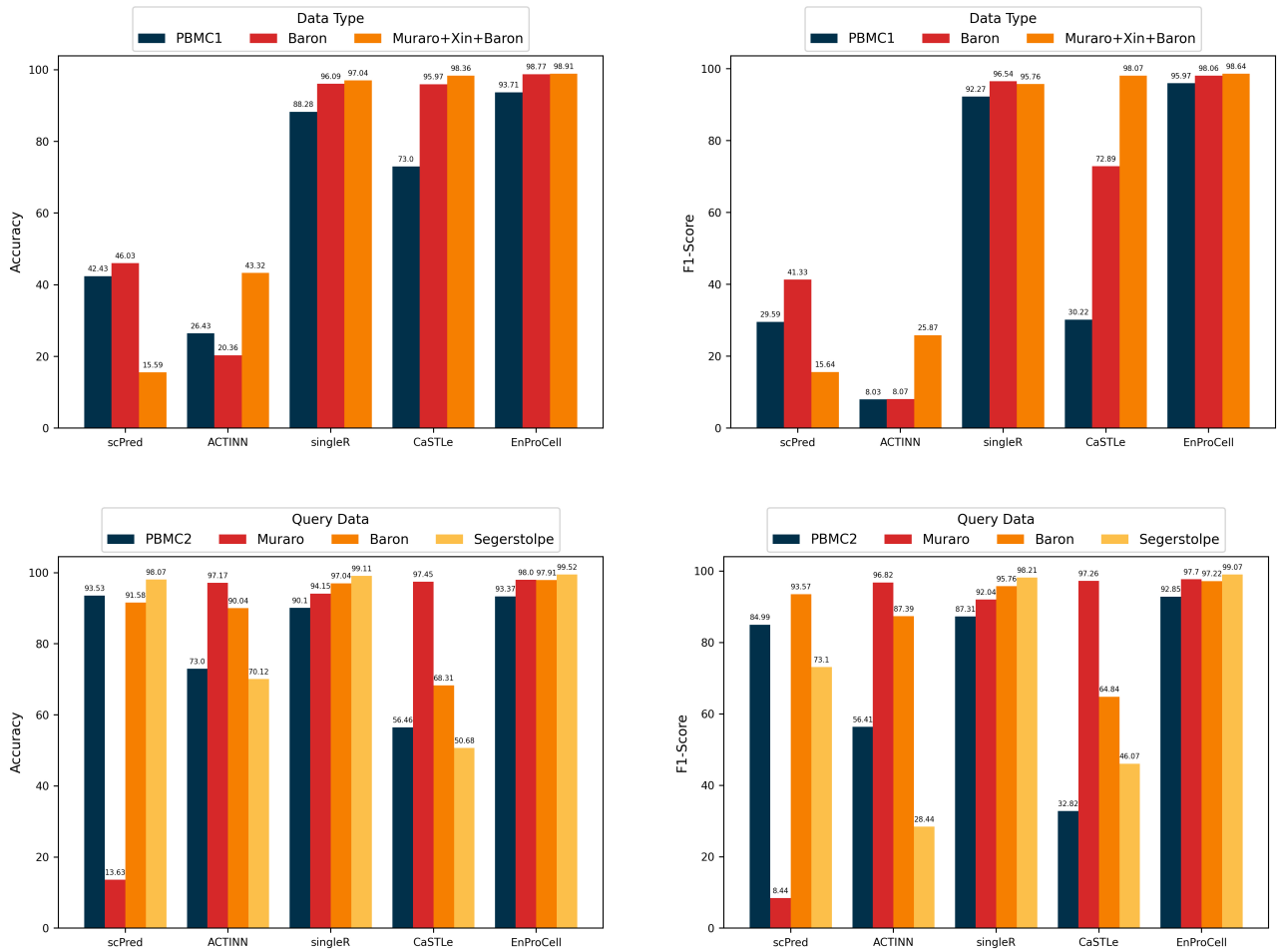


**Fig. 4.** (a) Accuracy of different classifiers on reference to reference prediction. (b) F1 score of different classifiers on reference to reference prediction. (c) Accuracy of different classifiers for reference to query prediction (d) F1 score of different classifiers for reference to query prediction.

score (95.97%) for PBMC1 data compared to other state-of-the-art methods. SingleR was the second-best-performing method for cell type classifications of PBMCs. For the Baron dataset, EnProCell showed the highest accuracy (98.77%), with the highest F1 score (98.06%). CaSTLe was ranked third and singleR was ranked second in the case of the Baron dataset. EnProCell, SingleR, and CaSTLe reported a comparable performance for a combined dataset of Muraro, Xin, and Baron as shown in Figure 4(a). ACTINN, NN-based method, and scPred, SVD-based method failed to achieve comparable performance in predicting the reference test data from the trained reference instances.

### Predicting the query cell types from reference scRNA data

The methods performing reasonably on reference data were further compared by their ability to predict query datasets with unknown cell types. The query datasets were not included in methods training and testing. In such cases, EnProCell utilizes the reference dataset to extract the principle components and to train the model while the query dataset is used for prediction. Furthermore, the Harmony algorithm (38) was employed to

remove the batch effect between the reference and query datasets.

At first human pancreatic (Muraro, Xin, Segerstolpe, and Baron) datasets were used to test the performance of EnProCell and other state-of-the-art methods. To create the reference and query dataset, one or multiple datasets were chosen randomly and were used as a reference and the remaining dataset was considered a query. For example, in the first experiment, Muraro was used as the query and the combined form of the other three datasets is used for training the model. There were three common cell types (alpha, beta, and delta) between these two datasets. The common cell types were selected from each dataset.

First, 2000 highly variable genes were selected from at least two of three datasets combined for training then the intersecting genes between these datasets were used for further analysis. After extracting the variable and common genes between the datasets three datasets are combined into a single matrix and then the PCA and MDA. The components extracted are ensembled and are used to project the training data and query in the lower dimensional space. The harmony algorithm is used to remove the batch effect as all the data sets are obtained using different protocols. The neural network is trained using the lower dimensional representation of reference data and then

the trained model is used to predict the query Muraro data. EnProCell showed the highest accuracy (98.00%) and F1 score (97.70) as shown in Figures 4(c) and 4(d) respectively. CaSTLe was the second best-performing classifier with a 97.45 percent accuracy and 97.26 percent F1 score. ACTINN was the third best-performing classifier.

In the second experiment Muraro, Xin, and Segerstolpe were combined to create the reference. The neural network was trained on created reference and cell types of the Baron dataset were predicted. Our method outperforms the other methods with 97.91 percent accuracy and 97.22 percent F1 score. In the third experiment Muraro, Xin, and Baron were used for training and Segerstolpe was considered as a query. In this experiment EnProCell showed better performance and the singleR and scPred were the second and third best-performing classifiers, as shown in Figure 4(c). In all experiments, evaluation measures showed that our proposed methodology outperforms the existing state-of-the-art methods.

For PBMC data, the model is trained on the blood cells from one individual (PBMC1) and for prediction using the data from another individual (PBMC2). PBMC1 is used as a reference and PBMC2 as the query. There were 9 common cell types between both datasets. EnProCell showed a 93.37 percent accuracy and a 92.85 percent F1 score. scPred showed better accuracy (93.53) with the F1 score of 84.99 but the F1 score of singleR and EnProCell was greater than scPred. In this experiment, CaSTLe showed the lowest accuracy and F1 score Figure 4(c).

## Comparison of test time

We compared the test time of our proposed methodology and the other methods for single-cell classification. The execution time was computed using the system with a 1.10 GHz, Intel Core i7 CPU with 32GB memory. Figure 5 shows the execution time for test data of different classifiers and our methodology for three different datasets. Our algorithm is 2.5, 13.7, and 2.6 times faster than the existing best algorithm which is CaSTLe for three different datasets PBMC1, Baron, and a combined data (Muraro, Xin, and Baron) respectively.

## Conclusion

The study presents a novel methodology, named as EnProCell to further improve cell type classification from scRNA-seq data. The first component of the proposed methodology is an ensemble of PCA and MDA, which aims to obtain discriminative features from cellular expression profiles. The second component trains an auto-encoder neural architecture on extracted discriminative features for cell type classification. EnProCell outperformed the existing state-of-the-art methods belonging to different data analytical techniques such as transfer learning. Furthermore, the performance of EnProCell was independent from the platform or technology used to produce the scRNA-seq data. The proposed deep architecture, trained on ensemble projections showed better performance on datasets belonging to different tissues and organisms. The results demonstrated that the method outperforms existing methods in terms of accuracy and F1 score, while also providing insights into the major sources of variability in scRNA-seq data. EnProCell requires less computational resources and has low computational complexity. Therefore, it can facilitate the

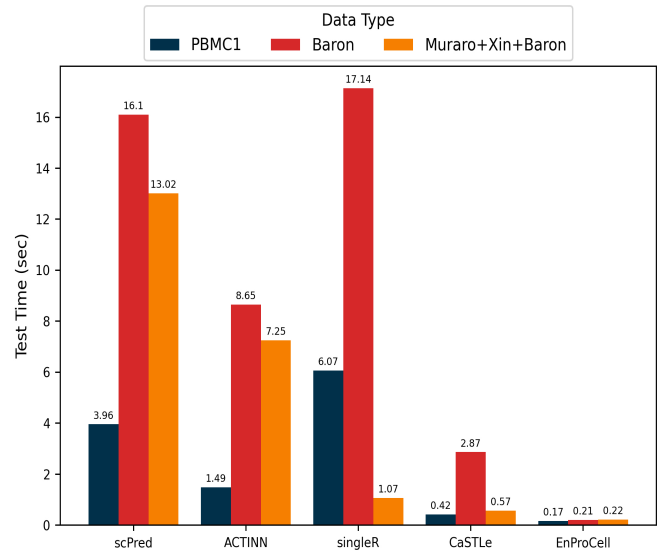


**Fig. 5.** Test time comparison of different methods used in the study using the different datasets. Time is reported for the test set cell label predictions.

discovery of novel cell types and bio-markers, and improve understanding of complex biological systems.

## Key points

- Single-cell RNA sequencing (scRNA-seq) enabled the study of complex biological mechanisms such as development and human organogenesis at the single-cell level
- The delineation of cell type specifications from sparse and high dimensional data of scRNA-seq can shed light on underlying cellular diversity
- In this study, we propose a novel method, EnProCell, for efficient and effective cell type classification in scRNA-seq data.
- EnProCell outperformed the existing state-of-the-art methods in classifying the cells from four different datasets

## References

1. Byungjin Hwang, Ji Hyun Lee, and Duhee Bang. Single-cell rna sequencing technologies and bioinformatics pipelines. *Experimental & molecular medicine*, 50(8):1–14, 2018.
2. Jin Sung Jang, Ying Li, Amit Kumar Mitra, Lintao Bi, Alexej Abyzov, Andre J van Wijnen, Linda B Baughn, Brian Van Ness, Vincent Rajkumar, Shaji Kumar, et al. Molecular signatures of multiple myeloma progression through single cell rna-seq. *Blood cancer journal*, 9(1):2, 2019.
3. Nobuyuki Tanaka, Shintaro Katayama, Aparna Reddy, Kaneyasu Nishimura, Naoya Niwa, Hiroshi Hongo, Koichiro Oghihara, Takeo Kosaka, Ryuichi Mizuno, Eiji Kikuchi, et al. Single-cell rna-seq analysis reveals the platinum resistance gene *cox7b* and the surrogate marker *cd63*. *Cancer medicine*, 7(12):6193–6204, 2018.
4. Livnat Jerby-Arnon, Parin Shah, Michael S Cuoco, Christopher Rodman, Mei-Ju Su, Johannes C Melms, Rachel Leeson, Abhay Kanodia, Shaolin Mei, Jia-Ren Lin,

- et al. A cancer cell program promotes t cell exclusion and resistance to checkpoint blockade. *Cell*, 175(4):984–997, 2018.
5. Yael C Cohen, Mor Zada, Shuang-Yin Wang, Chamutal Bornstein, Eyal David, Adi Moshe, Baoguo Li, Shir Shlomi-Loubaton, Moshe E Gatt, Chamutal Gur, et al. Identification of resistance pathways and therapeutic targets in relapsed multiple myeloma patients through single-cell sequencing. *Nature medicine*, 27(3):491–503, 2021.
  6. Fenna M Krienen, Melissa Goldman, Qiangge Zhang, Ricardo CH del Rosario, Marta Florio, Robert Machold, Arpiar Saunders, Kirsten Levandowski, Heather Zaniewski, Benjamin Schuman, et al. Innovations present in the primate interneuron repertoire. *Nature*, 586(7828):262–269, 2020.
  7. Laufey Geirsdottir, Eyal David, Hadas Keren-Shaul, Assaf Weiner, Stefan Cornelius Bohlen, Jana Neuber, Adam Balic, Amir Giladi, Fadi Sheban, Charles-Antoine Dutertre, et al. Cross-species single-cell analysis reveals divergence of the primate microglia program. *Cell*, 179(7):1609–1622, 2019.
  8. Takahiro Masuda, Roman Sankowski, Ori Staszewski, Chotima Böttcher, Lukas Amann, N Sagar, Christian Scheiwe, Stefan Nessler, Patrik Kunz, Geert van Loo, et al. Spatial and temporal heterogeneity of mouse and human microglia at single-cell resolution. *Nature*, 566(7744):388–392, 2019.
  9. Sueli Marques, David van Bruggen, Darya Pavlovna Vanichkina, Elisa Mariagrazia Floriddia, Hermany Munguba, Leif Våremo, Stefania Giacomello, Ana Mendanha Falcao, Mandy Meijer, Åsa Kristina Björklund, et al. Transcriptional convergence of oligodendrocyte lineage progenitors during development. *Developmental cell*, 46(4):504–517, 2018.
  10. Alexandra-Chloé Villani, Rahul Satija, Gary Reynolds, Siranush Sarkizova, Karthik Shekhar, James Fletcher, Morgane Griesbeck, Andrew Butler, Shiwei Zheng, Suzan Lazo, et al. Single-cell rna-seq reveals new types of human blood dendritic cells, monocytes, and progenitors. *Science*, 356(6335):eaah4573, 2017.
  11. Jong-Eun Park, Rachel A Botting, Cecilia Domínguez Conde, Dorin-Mirel Popescu, Marieke Lavaert, Daniel J Kunz, Issac Goh, Emily Stephenson, Roberta Ragazzini, Elizabeth Tuck, et al. A cell atlas of human thymic development defines t cell repertoire formation. *Science*, 367(6480):eaay3224, 2020.
  12. Itay Tirosh, Andrew S Venteicher, Christine Hebert, Leah E Escalante, Anoop P Patel, Keren Yizhak, Jonathan M Fisher, Christopher Rodman, Christopher Mount, Mariella G Filbin, et al. Single-cell rna-seq supports a developmental hierarchy in human oligodendrogloma. *Nature*, 539(7628):309–313, 2016.
  13. Itay Tirosh, Andrew S Venteicher, Christine Hebert, Leah E Escalante, Anoop P Patel, Keren Yizhak, Jonathan M Fisher, Christopher Rodman, Christopher Mount, Mariella G Filbin, et al. Single-cell rna-seq supports a developmental hierarchy in human oligodendrogloma. *Nature*, 539(7628):309–313, 2016.
  14. Fenna M Krienen, Melissa Goldman, Qiangge Zhang, Ricardo CH del Rosario, Marta Florio, Robert Machold, Arpiar Saunders, Kirsten Levandowski, Heather Zaniewski, Benjamin Schuman, et al. Innovations present in the primate interneuron repertoire. *Nature*, 586(7828):262–269, 2020.
  15. Aviv Regev, Sarah A Teichmann, Eric S Lander, Ido Amit, Christophe Benoist, Ewan Birney, Bernd Bodenmiller, Peter Campbell, Piero Carninci, Menna Clatworthy, et al. The human cell atlas. *elife*, 6:e27041, 2017.
  16. Dvir Aran, Agnieszka P Looney, Leqian Liu, Esther Wu, Valerie Fong, Austin Hsu, Suzanna Chak, Ram P Naikawadi, Paul J Wolters, Adam R Abate, et al. Reference-based analysis of lung single-cell sequencing reveals a transitional profibrotic macrophage. *Nature immunology*, 20(2):163–172, 2019.
  17. Jose Alquicira-Hernandez, Anuja Sathe, Hanlee P Ji, Quan Nguyen, and Joseph E Powell. scpred: accurate supervised method for cell-type classification from single-cell rna-seq data. *Genome biology*, 20(1):1–17, 2019.
  18. Yuval Lieberman, Lior Rokach, and Tal Shay. Castle-classification of single cells by transfer learning: harnessing the power of publicly available single cell rna sequencing experiments to annotate new experiments. *PLoS one*, 13(10):e0205499, 2018.
  19. Feiyang Ma and Matteo Pellegrini. Actinn: automated identification of cell types in single cell rna sequencing. *Bioinformatics*, 36(2):533–538, 2020.
  20. Vladimir Yu Kiselev, Kristina Kirschner, Michael T Schaub, Tallulah Andrews, Andrew Yiu, Tamir Chandra, Kedar N Natarajan, Wolf Reik, Mauricio Barahona, Anthony R Green, et al. Sc3: consensus clustering of single-cell rna-seq data. *Nature methods*, 14(5):483–486, 2017.
  21. Andrew Butler, Paul Hoffman, Peter Smibert, Eftymia Papalexi, and Rahul Satija. Integrating single-cell transcriptomic data across different conditions, technologies, and species. *Nature biotechnology*, 36(5):411–420, 2018.
  22. Justina Žurauskienė and Christopher Yau. pcreduce: hierarchical clustering of single cell transcriptional profiles. *BMC bioinformatics*, 17:1–11, 2016.
  23. Xinxin Zhang, Yujia Lan, Jinyuan Xu, Fei Quan, Erjie Zhao, Chunyu Deng, Tao Luo, Liwen Xu, Gaoming Liao, Min Yan, et al. Cellmarker: a manually curated resource of cell markers in human and mouse. *Nucleic acids research*, 47(D1):D721–D728, 2019.
  24. Tabula Muris Consortium, Overall coordination Schaum Nicholas 1 Karkanas Jim 2 Neff Norma F. 2 May Andrew P. 2 Quake Stephen R. quake@stanford.edu 2 3 f Wyss-Coray Tony twc@stanford.edu 4 5 6 g Darmanis Spyros spyros.darmanis@czbiohub.org 2 h, Logistical coordination Batson Joshua 2 Botvinnik Olga 2 Chen Michelle B. 3 Chen Steven 2 Green Foad 2 Jones Robert C. 3 Maynard Ashley 2 Penland Lolita 2 Pisco Angela Oliveira 2 Sit Rene V. 2 Stanley Geoffrey M. 3 Webber James T. 2 Zanini Fabio 3, and Computational data analysis Batson Joshua 2 Botvinnik Olga 2 Castro Paola 2 Croote Derek 3 Darmanis Spyros 2 DeRisi Joseph L. 2 27 Karkanas Jim 2 Pisco Angela Oliveira 2 Stanley Geoffrey M. 3 Webber James T. 2 Zanini Fabio 3. Single-cell transcriptomics of 20 mouse organs creates a tabula muris. *Nature*, 562(7727):367–372, 2018.
  25. Oscar Franzén, Li-Ming Gan, and Johan LM Björkegren. PanglaoDB: a web server for exploration of mouse and human single-cell rna sequencing data. *Database*, 2019:baz046, 2019.
  26. Karl Weiss, Taghi M Khoshgoftaar, and DingDing Wang. A survey of transfer learning. *Journal of Big data*, 3(1):1–40, 2016.

27. Xiaoxiao Guo, Wei Li, and Francesco Iorio. Convolutional neural networks for steady flow approximation. In *Proceedings of the 22nd ACM SIGKDD international conference on knowledge discovery and data mining*, pages 481–490, 2016.
28. Vladimir Yu Kiselev, Tallulah S Andrews, and Martin Hemberg. Challenges in unsupervised clustering of single-cell rna-seq data. *Nature Reviews Genetics*, 20(5):273–282, 2019.
29. Andrew Butler, Paul Hoffman, Peter Smibert, Efthymia Papalexi, and Rahul Satija. Integrating single-cell transcriptomic data across different conditions, technologies, and species. *Nature biotechnology*, 36(5):411–420, 2018.
30. F Alexander Wolf, Philipp Angerer, and Fabian J Theis. Scanpy: large-scale single-cell gene expression data analysis. *Genome biology*, 19:1–5, 2018.
31. Vladimir Yu Kiselev, Kristina Kirschner, Michael T Schaub, Tallulah Andrews, Andrew Yiu, Tamir Chandra, Kedar N Natarajan, Wolf Reik, Mauricio Barahona, Anthony R Green, et al. Sc3: consensus clustering of single-cell rna-seq data. *Nature methods*, 14(5):483–486, 2017.
32. Dvir Aran, Agnieszka P Looney, Leqian Liu, Esther Wu, Valerie Fong, Austin Hsu, Suzanna Chak, Ram P Naikawadi, Paul J Wolters, Adam R Abate, et al. Reference-based analysis of lung single-cell sequencing reveals a transitional profibrotic macrophage. *Nature immunology*, 20(2):163–172, 2019.
33. Maayan Baron, Adrian Veres, Samuel L Wolock, Aubrey L Faust, Renaud Gaujoux, Amedeo Vetere, Jennifer Hyoje Ryu, Bridget K Wagner, Shai S Shen-Orr, Allon M Klein, et al. A single-cell transcriptomic map of the human and mouse pancreas reveals inter-and intra-cell population structure. *Cell systems*, 3(4):346–360, 2016.
34. Mauro J Muraro, Gitanjali Dharmadhikari, Dominic Grün, Nathalie Groen, Tim Dielen, Erik Jansen, Leon Van Gorp, Marten A Engelse, Françoise Carlotti, Eelco Jp De Koning, et al. A single-cell transcriptome atlas of the human pancreas. *Cell systems*, 3(4):385–394, 2016.
35. Åsa Segerstolpe, Athanasia Palasantza, Pernilla Eliasson, Eva-Marie Andersson, Anne-Christine Andréasson, Xiaoyan Sun, Simone Picelli, Alan Sabirsh, Maryam Clausen, Magnus K Bjursell, et al. Single-cell transcriptome profiling of human pancreatic islets in health and type 2 diabetes. *Cell metabolism*, 24(4):593–607, 2016.
36. Yurong Xin, Jinrang Kim, Haruka Okamoto, Min Ni, Yi Wei, Christina Adler, Andrew J Murphy, George D Yancopoulos, Calvin Lin, and Jesper Gromada. Rna sequencing of single human islet cells reveals type 2 diabetes genes. *Cell metabolism*, 24(4):608–615, 2016.
37. Anne Senabouth, Stacey Andersen, Qianyu Shi, Lei Shi, Feng Jiang, Wenwei Zhang, Kristof Wing, Maciej Daniszewski, Samuel W Lukowski, Sandy SC Hung, et al. Comparative performance of the bgi and illumina sequencing technology for single-cell rna-sequencing. *NAR genomics and bioinformatics*, 2(2):lqaa034, 2020.
38. Ilya Korsunsky, Nghia Millard, Jean Fan, Kamil Slowikowski, Fan Zhang, Kevin Wei, Yuriy Baglaenko, Michael Brenner, Po-ru Loh, and Soumya Raychaudhuri. Fast, sensitive and accurate integration of single-cell data with harmony. *Nature methods*, 16(12):1289–1296, 2019.